

Realizing universal topological quantum gates in simulated time-reversal-invariant superconducting chains

Yong Hu,^{1,2,*} Y. X. Zhao,¹ Zheng-Yuan Xue,¹ and Z. D. Wang^{1,†}

¹*Department of Physics and Center of Theoretical and Computational Physics,
The University of Hong Kong, Pokfulam Road, Hong Kong, China*

²*School of Physics, Huazhong University of Science and Technology, Wuhan, 430074, China*

We propose a topology-preserved hard-core boson simulator of one-dimensional time-reversal-invariant topological superconductor. By using the developed dispersive dynamic modulation approach, not only the faithful simulation of this DIII type of spinful superconducting chains is achieved, but also a set of universal topological quantum gates can be realized. Physical implementation of our scheme based on a Josephson quantum circuit is presented, where our detailed analysis pinpoints that this scheme is experimentally feasible with the state-of-the-art technology.

PACS numbers: 03.67.Lx, 03.65.Vf, 85.25.-j

Introduction—In exploration of symmetry-protected topological phases, more and more attention has been drawn to theoretical and experimental studies of topological superconducting wires in the symmetry class DIII [1–7]. In contrast to the Kitaev model in the class D with one Majorana zero mode (MZM) at each end and two-fold degenerate ground states in its $\mathbb{Z}_2^{(1)}$ topological phase [8], the DIII superconductor wire in the $\mathbb{Z}_2^{(2)}$ topological phase protected by the time-reversal symmetry (TRS) has a Kramers doublet of MZMs at each end and four-fold degenerate ground states [9]. Moreover, the DIII superconductor wire may exhibit an impactful response to an effective magnetic field and long-range spin-correlation at the two ends with the fixed fermionic parity, which can be utilized to realize universal quantum operations of topological qubits [2, 5, 6]. Although being studied theoretically, still the one-dimensional TRS protected \mathbb{Z}_2 topological phase has not been tested experimentally so far.

On the other hand, it has been indicated that one-dimensional (1D) hard-core boson (HCB) chain may be able to simulate fermionic physics [10], with interesting phenomena being investigated including the pursuit of Majorana fermions in the Kitaev model [11–13], the string breaking dynamics of quark pairs [14], and the electron-electron scattering [15]. However, methods in the existing studies are restricted to spinless fermions, where the forms of the concerned Hamiltonians remain unchanged during the bosonization. When bosonizing a spinful 1D fermionic system, an exotic particle-density-dependent $U(1)$ gauge field emerges from fermionic statistics among fermions with opposite spin orientations, leading to one of main challenges in the simulation of the spinful DIII models.

In this Letter, we reveal unambiguously that a 1D HCB lattice can be exploited to faithfully simulate the proposed DIII model which realizes the nontrivial $\mathbb{Z}_2^{(2)}$ topological phase [5]. Most remarkably, with the odd-parity Kramers doublet ground states being used as the basis

of topological qubits, we demonstrate for the first time that a set of universal topological quantum gates can in principle be achieved with the help of this HCB architecture, where we develop a dispersive dynamic modulation (DDM) approach to mediate the exotic $U(1)$ gauge field configuration in the bosonized DIII model. Moreover, we propose a physical implementation scheme based on superconducting quantum circuit (SQC) [16, 17]. Taking the advantages of flexibility and scalability of SQC [18, 19], we encode HCBs by superconducting transmon qubits and design the nontrivial coupling through the inductive connection between transmon qubits [20–23]. Our estimation also implies that the effective coupling strengths can be several orders larger than the decoherence rates of the transmon qubits [24, 25], and therefore the proposed topological operations may be tested with the current level of technology.

The HCB realization of DIII model—An intriguing model Hamiltonian of fermionic 1D topological superconductor in the class DIII reads [5],

$$H_{\text{DIII}} = \sum_{j\alpha} (-wc_{j,\alpha}^\dagger c_{j+1,\alpha} - i\Delta c_{j+1,\alpha} c_{j,\bar{\alpha}} + \text{h.c.}) - \mu(c_{j,\alpha}^\dagger c_{j,\alpha} - 1) \quad (1)$$

where $c_{j,\alpha}^\dagger$ is the creation operator of the spin- α fermion on the j th site with $\alpha = \uparrow, \downarrow$ and Δ is the real-value amplitude of p-wave pairing parameter. Under the basis transformation $a_j = e^{-i\pi/4}(c_{j,\uparrow} + c_{j,\downarrow})/\sqrt{2}$ and $\bar{a}_j = e^{-i\pi/4}(c_{j,\uparrow} - c_{j,\downarrow})/\sqrt{2}$, H_{DIII} can be rewritten as

$$H_{\text{DIII}} = H + \bar{H}$$

with

$$H = \sum_j (-wa_j^\dagger a_{j+1} + \Delta a_{j+1} a_j + \text{h.c.}) - \mu(a_j^\dagger a_j - 1/2) \\ \bar{H} = \sum_j (-w\bar{a}_j^\dagger \bar{a}_{j+1} - \Delta \bar{a}_{j+1} \bar{a}_j + \text{h.c.}) - \mu(\bar{a}_j^\dagger \bar{a}_j - 1/2) \quad (2)$$

i.e., H_{DIII} is decoupled into two Kitaev chains differed by the signs of their superconducting order parameters

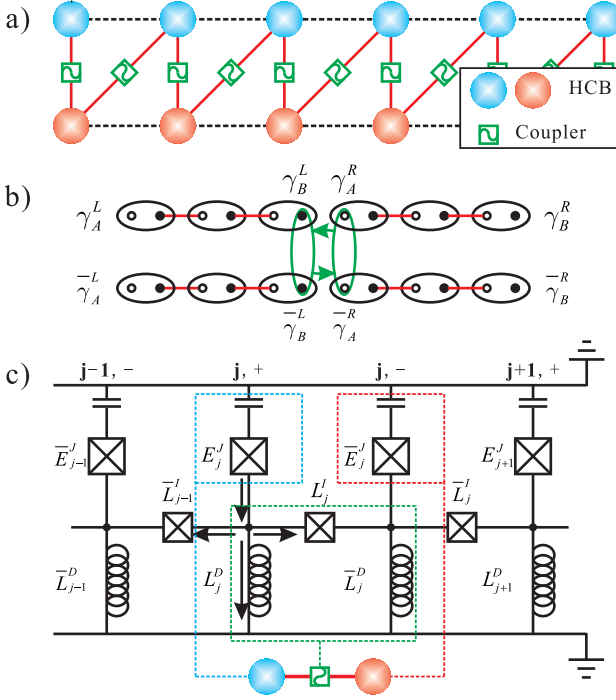


FIG. 1: (a) Schematic view of the 1-D HCB simulator of H_{DIII} . The solid red line describes the path along which the HCB sites are physically coupled and the bosonization is performed. Through the DDM of the nearest neighbor coupling (the green wavelet boxes) the effective intra-species hopping and pairing (the black dashed lines) can be induced. The 12-HCB lattice shown is minimal for the demonstration of universal quantum operations. (b) Realization of nontrivial two-qubit gate in the 12-HCB lattice. In the situation $w = \Delta$ and $\mu = 0$, each HCB site (the ellipse) can be decomposed into two Majorana modes (the filled and the hollow dots) pairing in the bulk. Two topological qubits can be prepared by “cutting” the whole DIII chain into two pieces. Through the modulation of $(3, -) \longleftrightarrow (4, +)$ coupling, the effective $\gamma_B^L \gamma_A^R + \bar{\gamma}_B^L \bar{\gamma}_A^R$ coupling can be induced. (c) Schematic plot of the array of coupled transmon qubits.

(hereafter we denote the quantities related with the $(+)$ -chain as A and their counterparts for the $(-)$ -chain as \bar{A}). Although the topology-preserved simulation of a standard Kitaev model with HCBs has been proposed [11–13], to simulate H_{DIII} with HCBs is much more challenging than the separate simulations of H^+ and H^- by two independent HCB chains, because such straightforward scenario cannot result in the fermionic anti-commutation relation of inter-species. For this, here we exploit a quasi-1D HCB chain shown in Fig.1(a), where the upper/lower array plays the role of the $+/-$ chain, respectively. The DIII model (2) can be bosonized as

$$H = \sum_j (-w \bar{P}_j b_j^\dagger b_{j+1} + \Delta \bar{P}_j b_{j+1} b_j + \text{h.c.}) - \mu (b_j^\dagger b_j - \frac{1}{2})$$

$$\bar{H} = \sum_j (-w P_{j+1} \bar{b}_j^\dagger \bar{b}_{j+1} - \Delta P_{j+1} \bar{b}_{j+1} \bar{b}_j + \text{h.c.}) - \mu (\bar{b}_j^\dagger \bar{b}_j - \frac{1}{2}) \quad (3)$$

with the bosonization along the zig-zag path in Fig. 1(a) being given by $b_j = a_j \prod_{s < j} P_s \prod_{s < j} \bar{P}_s$ and $\bar{b}_j = \bar{a}_j \prod_{s < j+1} P_s \prod_{s < j} \bar{P}_s$. Here $b_j(\bar{b}_j)$ is the anni-

hilation operators of the j th HCB on the $(+)(-)$ chain, $P_s = \exp(-i\pi a_s^\dagger a_s) [= \exp(-i\pi b_s^\dagger b_s)]$, and $\bar{P}_s = \exp(-i\pi \bar{a}_s^\dagger \bar{a}_s)$ [26]. It is noticed that the fermionic anti-commutation relation has been converted to the gauge field factors after bosonization, which in one chain is given by the particle density of the other chain in a site-wise sense.

To implement the bosonization version of the DIII model (3), we set that the HCBs on the upper/lower array of Fig.1(a) have energy splits $\Omega/\bar{\Omega}$ with $\delta = \Omega - \bar{\Omega} \sim 0.3\Omega$, and the inter-HCB coupling takes the nearest-neighbor form $H^L = \sum_j \mathcal{H}_j^L + \bar{\mathcal{H}}_j^L$ with $\mathcal{H}_j^L = V_j(t)(b_j^\dagger + b_j)(\bar{b}_j^\dagger + \bar{b}_j)$ and $\bar{\mathcal{H}}_j^L = \bar{V}_j(t)(\bar{b}_j^\dagger + \bar{b}_j)(b_{j+1}^\dagger + b_{j+1})$ where $|V_j(t)|, |\bar{V}_j(t)| \sim 10^{-2}\delta$ are the coupling strengths which can be modulated harmonically and *in situ*. We further introduce a dispersive energy threshold $\eta \sim 10^{-1}\delta$ such that $|V_j(t)|, |\bar{V}_j(t)| \ll \eta \ll \delta$ and modulate $V_j(t)$ and $\bar{V}_j(t)$ as

$$V_j(t) = 2t_j \cos(\eta - \delta)t + 2q_j \cos(\eta - \epsilon)t$$

$$\bar{V}_j(t) = 2\bar{t}_j \cos(\eta - \delta)t + 2\bar{q}_j \cos(\eta + \epsilon)t \quad (4)$$

with $\epsilon = \Omega + \bar{\Omega}$. Based on the parameter choice

$$t_j = (-1)^{j-1}t, q_j = (-1)^{j-1}q$$

$$\bar{t}_j = (-1)^{j-1}\bar{t}, \bar{q}_j = (-1)^{j-1}\bar{q}, \bar{q}/\bar{t} = -q/t \quad (5)$$

we can directly reproduce the hopping and pairing terms in Eq.(3) with $w = -t\bar{t}/\eta$ and $\Delta = t\bar{q}/\eta$ from the dispersive coupling between $\sum_j \mathcal{H}_j^L$ and $\sum_j \bar{\mathcal{H}}_j^L$ [27]. The obtained amplitudes of w and Δ can be independently tuned in the range $[10^{-3}, 10^{-2}]\delta$ by the parameters (t, q, \bar{t}, \bar{q}) . In addition, the chemical potential term in Eq.(3) can be produced by adding an on-site dispersive radiation $H^D = \sum_j D_j(t)(b_j^\dagger + b_j) + \bar{D}_j(t)(\bar{b}_j^\dagger + \bar{b}_j)$. A convenient choice of $D_j(t)$ (and similarly $\bar{D}_j(t)$) is $D_j(t) = d_j[e^{i(\Omega \pm 3\eta)} + e^{-i(\Omega \pm 3\eta)}]$ which results in the a.c. Stark shift $\pm d_j^2 b_j^\dagger b_j / 3\eta$. The 3η setting of the radiation frequency is to avoid the crosstalk between H^D and H^L , and the choice of the 3η sign depends on whether positive or negative correction of the chemical potential is needed.

MZMs and the universal quantum gates—The region $|w| > |\mu/2|$ can be identified as the topological phase where the nontrivial MZMs emerge [8]. Especially, we focus on the ideal case $w = \Delta$ and $\mu = 0$ where the DIII model (2) can simply be reduced to

$$H_{DIII} = \sum_j i w (\gamma_{j,B} \gamma_{j+1,A} + \bar{\gamma}_{j,B} \bar{\gamma}_{j+1,A}), \quad (6)$$

with Majorana operators $\gamma_{j,A} = i(a_j - a_j^\dagger)$, $\gamma_{j,B} = a_j + a_j^\dagger$, $\gamma_{j,A} = \bar{a}_j + \bar{a}_j^\dagger$, and $\gamma_{j,B} = -i(\bar{a}_j - \bar{a}_j^\dagger)$. The Hamiltonian is fully diagonalized through the pairing of $\gamma_{j,B}$ and $\gamma_{j+1,A}$ (and simultaneously $\bar{\gamma}_{j,B}$ and $\bar{\gamma}_{j+1,A}$) in the bulk, leaving four MZMs $\gamma_A = \gamma_{1,A}$,

$\bar{\gamma}_A = \bar{\gamma}_{1,A}$, $\gamma_B = \gamma_{N,B}$, and $\bar{\gamma}_B = \bar{\gamma}_{N,B}$ unpaired at the two ends (N being the length of the DIII chain). The ground states are thus four-fold degenerate with a basis $\{|1\rangle|\bar{1}\rangle, |0\rangle|\bar{0}\rangle, |1\rangle|\bar{0}\rangle, |0\rangle|\bar{1}\rangle\}$ satisfying $-i\gamma_A\gamma_B|0, 1\rangle = \pm|0, 1\rangle$ and $-i\bar{\gamma}_A\bar{\gamma}_B|\bar{0}, \bar{1}\rangle = \pm|\bar{0}, \bar{1}\rangle$. Here we choose the ground subspace spanned by $|\bullet\rangle = |0\rangle|\bar{1}\rangle$ and $|\times\rangle = |1\rangle|\bar{0}\rangle$ as a topological qubit. Such subspace has odd parity distinguishing it from the other ground states. For comparison, we recall that the ground state of the Kitaev model with only one Majorana zero mode at each end have the opposite (even) fermionic parity [8].

Since a single Kitaev chain can be minimally simulated by a 3-HCB array [12], for an easy experimental setup but without loss of generality, below we consider a 12-HCB lattice to demonstrate the universal topological quantum operations. As sketched in Fig.1(b), we notice that two DIII chains can be constructed by the 12-HCB lattice: we “cut” the whole chain into two pieces by tuning $\bar{t}_3 = \bar{q}_3 = 0$ and $q_4 = 0$ [28]. The 12-HCB chain is thus decomposed into two subchains labeled by L and R, with 8 emerged MZMs (4 for each subchain), as shown in Fig.1(b). For each subchain, the previously established formalism of defining topological qubits can still be exploited. For universal single qubit operation, we take the left subchain as an example by considering $H_S = \mathbf{B} \cdot \hat{\mathbf{S}}^L$ with \mathbf{B} as an effective magnetic field, which is very weak compared with the bulk gap, and $\hat{\mathbf{S}}^L = \sum_{j=1}^3 (a_j^\dagger, \bar{a}_j^\dagger) \hat{\sigma} (a_j, \bar{a}_j)^T$. It has been shown that $\hat{\mathbf{S}}^L$ can be regarded as an effective single spin operator acting on the left topological qubit, with $|\bullet\rangle^L$ and $|\times\rangle^L$ being the two eigenstates of \hat{S}_z^L [5]. Thus through the control of \mathbf{B} the universal single-qubit operation can be achieved. The \mathbf{S}_x^L rotation can be implemented by the resonant dynamic modulation approach: for each $(j, +) \longleftrightarrow (j, -)$ link, we add a resonant tone $V_j^{\text{RX}}(t) = 2B_x(t) \cos \delta t$ to $V_j(t)$ with $B_x(t)$ the slow-varying (adiabatic) pulse amplitude satisfying $B_x(t_i) = B_x(t_f) = 0$ to induce the resonant inter-species hopping $\sum_{j=1}^3 B_x(t) (b_j^\dagger \bar{b}_j + b_j \bar{b}_j^\dagger)$ which is equivalent to $H_{\text{SX}} = B_x(t) \mathbf{S}_x^L$ in the fermionic picture. The rotation $\exp(-i\theta \mathbf{S}_x^L)$ with $\theta = \int_{t_i}^{t_f} B_x dt$ can be realized after t_f . The \mathbf{S}_y^L rotation can be similarly realized by changing the initial phase of the resonant dynamic modulation as $V_j^{\text{RY}}(t) = 2B_y(t) \cos(\delta t - \pi/2)$.

To implement the nontrivial inter-qubit quantum gate, we modulate $\bar{V}_3(t)$ as $\bar{V}_3(t) = 2\bar{h}(t) \cos(\eta - \delta)t$ to induce the effective $(3, +) \longleftrightarrow (4, +)$ and $(3, -) \longleftrightarrow (4, -)$ hopping which can be written as

$$H_M^T = -i \frac{t_M}{2} (\gamma_B^L \gamma_A^R + \bar{\gamma}_B^L \bar{\gamma}_A^R), \quad (7)$$

with $t_M = \bar{h}(t)/\eta$. The coupling strength t_M can be controlled by the slow-varying envelope $\bar{h}(t)$ such that $|t_M| \ll \Delta$, $t_M(0) = t_M(t_f) = 0$, and $\int_{t_i}^{t_f} t_M dt = \pi$. Consequently, we get an unitary transformation $U =$

$-\gamma_B^L \gamma_A^R \bar{\gamma}_B^L \bar{\gamma}_A^R$ transforming the four basis states as

$$\begin{aligned} |\bullet\rangle^L |\bullet\rangle^R &\rightarrow |\times\rangle^L |\times\rangle^R, & |\times\rangle^L |\bullet\rangle^R &\rightarrow -|\bullet\rangle^L |\times\rangle^R, \\ |\bullet\rangle^L |\times\rangle^R &\rightarrow -|\times\rangle^L |\bullet\rangle^R, & |\times\rangle^L |\times\rangle^R &\rightarrow |\bullet\rangle^L |\bullet\rangle^R, \end{aligned}$$

i.e., U acts as a nontrivial two-qubit gate $-\mathbf{S}_y^L \otimes \mathbf{S}_y^R$ which can be exploited to achieve a set of universal quantum gates in combination with the single-qubit gates mentioned previously.

Physical implementation with superconducting circuits—We now elaborate in detail how to implement the present theoretical scheme by SQCs. For the site $(j, +)$ we consider a superconducting transmon qubit consisting of a superconducting quantum interference device (SQUID) with effective Josephson energy E_j^J shunted by a large capacitance C_j [20, 21], as shown in Fig.1(c). The two characteristic energy scales of the transmon qubit are its anharmonicity $E_j^C = e^2/2C_j$ and its lowest level splitting $\Omega_j \simeq \sqrt{8E_j^C E_j^J}$. Here we choose j -independent $\Omega_j/2\pi = \Omega/2\pi = 20$ GHz and $E_j^C/2\pi \simeq 500$ MHz. The HCB sites on the ‘-’ chain can be similarly constructed with $\bar{\Omega}_j/2\pi = \bar{\Omega}/2\pi = 15$ GHz and $\bar{E}_j^C \simeq E_j^C$. Due to the large anharmonicity, the presence of the higher levels of the transmons can only slightly modify the effective parameters derived below and the transmons can be consequently modeled by the two-level HCB Hamiltonian $H^{\text{HCB}} = \sum_j \Omega b_j^\dagger b_j + \bar{\Omega} \bar{b}_j^\dagger \bar{b}_j$. For the links between neighboring qubits, we exploit the current divider technique recently studied in experiments [22, 23]. The transmon qubit design is slightly modified by introducing a small grounding inductance $L_j^D \simeq 5 \times 10^{-1} L_j^J$ with $L_j^J = \Phi_0^2/4\pi^2 E_j^J$ the effective inductance of the transmon SQUID at $(j, +)$. A low voltage node is thus created for each transmon qubit (Fig.1(c)), and the neighboring nodes are connected by coupling SQUIDs with tunable Josephson inductances $L_j^I, \bar{L}_j^I \simeq L_j^J/4$. Moreover, the capacitances of the coupling SQUIDs is chosen to be much smaller than C_j .

The inter-qubit coupling can be established by the current dividing mechanism. An excitation current from the $(j, +)$ qubit which can be written as $I_j \simeq \sqrt{\Omega/2L_j^J} (b_j^\dagger + b_j)$ will mostly flow through L_j^D to the ground, with a small fractions $I_{j+,j-}$ and $I_{j+,(j-1)-}$ flowing to the neighboring qubits $(j-1, -)$ and $(j, -)$ through the two coupling SQUIDs. The current $I_{j+,j-}$ in turn generates a flux $\Phi_{j+,j-} = \bar{L}_j^D I_{j+,j-}$ in the $(j, -)$ qubit. The interaction between the two qubits can thus be written as

$$\mathcal{H}_j^L = V_j (b_j^\dagger + b_j) (\bar{b}_j^\dagger + \bar{b}_j), \quad (8)$$

where the coupling constant V_j can be estimated as $V_j \simeq -(\Omega \bar{\Omega}/L_j^J \bar{L}_j^J)^{1/2} \bar{L}_j^D L_j^D / L_j^I$. Therefore, the a.c. modulation of the penetrating flux bias in the coupling SQUID loop results in the oscillation of L_j^I and in turn the oscillation of the inter-transmon coupling. Here we

should notice that the modulation frequencies of the coupling SQUIDS should not be higher than their plasma frequencies, otherwise complicated quasiparticle excitations would occur. As being mentioned previously, the maximal modulating frequency of the DDM approach is of the order $\epsilon = \Omega + \bar{\Omega}$. Therefore, with parameters being chosen before, this plasma frequency requirement is guaranteed by the small capacitance of the coupling SQUIDS.

The d.c. bias of the coupling SQUIDS leads to a static nearest neighbor qubit-qubit couplings which is estimated to be on the level of $2\pi[150, 200]$ MHz. Since such nearest-neighbor static coupling strength is much smaller than the energy difference between neighboring qubits (on the level of $2\pi \times 5$ GHz), its influence is the corrections of the hopping and pairing parameters derived from the DDM method. The couplings beyond the nearest neighbors should also be estimated: we notice that the divided current $I_{j+,j-}$ from $(j, +)$ qubit can be further divided in the $(j, -)$ node to flow through the $(j+1, +)$ node, thus the next-nearest-neighbor (NNN) $(j, +) \longleftrightarrow (j+1, +)$ static coupling is induced. Meanwhile, due to the current division mechanism at the low-voltage nodes, the non-nearest-neighbor couplings decay exponentially with respect to the site distance. The NNN coupling is estimated to be of the order $2\pi[30, 40]$ MHz. To suppress its effect we can use the two-sublattice strategy for each of the two HCB legs: the eigenfrequencies of the four qubits shown in Fig.1(c) can be modified to be $2\pi(15, 20, 14, 21)$ GHz, respectively. Such modification does not influence the performance of the DDM method as we merely need to adjust the modulating frequencies of $V_j(t)$ and $\bar{V}_j(t)$ accordingly. However, the effect of the d.c. NNN coupling is significantly suppressed by the 1 GHz energy difference between the NNN transmon qubits.

Based on the static bias, we can add the a.c. modulation pluses on the coupling SQUIDS with t, q, \bar{t}, \bar{q} at the order of $2\pi[50, 60]$ MHz and choose the dispersive active region as $\eta/2\pi = 300$ MHz. The resulting dispersive tunneling is estimated to be on the level $w/2\pi, \Delta/2\pi \in [10, 20]$ MHz which is three orders larger than the reported decoherence rates of the transmon qubits (in the range $2\pi[1, 10]$ kHz [24, 25]). Such strong tunnel/pairing allow us to set the slow varying envelopes on the level $B_x(t)/2\pi, B_y(t)/2\pi, t_M/2\pi \in [10^{-1}, 1]$ MHz. Following this setting, the envelopes are all much smaller than the realized bulk gap ($\Delta/2\pi \simeq 10$ MHz) such that the high energy excitations can be omitted, but stronger enough than the decoherence rates such that the proposed topological quantum operations can be simulated.

Conclusion—In conclusion, we have designed a topology-preserved HCB simulator for the TRS-invariant DIII topological superconducting chains and, most importantly, achieved for the first time a set of universal topological quantum gates through the developed DDM

technique. Physical implementation of our proposal with SQCs has been exploited. The present results may pave the way for realizing universal topological quantum computation.

Acknowledgments— We thank T. Mao and D. Zhang for helpful discussions. This work was supported in part by the GRF (HKU7058/11P&HKU7045/13P), the CRF (HKU8/11G) of Hong Kong, the National Science Foundation (NFS) of China (Grant No. 11104096 and No. 11374117), the National Fundamental Research Program of China (Grant Nos. 2011CB922104&2012CB922103). Y. Hu is supported by the fellowship of HongKong Scholars Program, Grant No. 2012-80.

* huyong@hku.hk

† zwang@hku.hk

- [1] C. L. M. Wong, and K. T. Law, Phys. Rev. B **86**, 184516 (2012).
- [2] S. Nakosai, J. C. Budich, Y. Tanaka, B. Trauzettel, and N. Nagaosa, Phys. Rev. Lett. **110**, 117002 (2013).
- [3] A. Keselman, L. Fu, A. Stern, and E. Berg, Phys. Rev. Lett. **111**, 116402 (2013).
- [4] F. Zhang, C. L. Kane, and E. J. Mele, Phys. Rev. Lett. **111**, 056402 (2013); Phys. Rev. Lett. **111**, 056403 (2013).
- [5] Y. X. Zhao and Z. D. Wang, Phys. Rev. B **90**, 115158 (2014).
- [6] E. Dumitrescu, J. D. Sau and S. Tewari, Phys. Rev. B **90**, 245438 (2014).
- [7] E. Gaidamauskas, J. Paaske, and K. Flensberg, Phys. Rev. Lett. **112**, 126402 (2014).
- [8] A. Y. Kitaev, Phys. Usp. **44**, 131 (2001).
- [9] Y. X. Zhao and Z. D. Wang, Phys. Rev. B **89**, 075111 (2014); Phys. Rev. Lett. **110**, 240404 (2013).
- [10] I. Carusotto, D. Gerace, H. E. Türeci, S. De Liberato, C. Ciuti, and A. Imamoglu, Phys. Rev. Lett. **103**, 033601 (2009).
- [11] C. E. Bardyn and A. Imamoglu, Phys. Rev. Lett. **109**, 253606 (2012).
- [12] J. Q. You, Z. D. Wang, W. Zhang, and F. Nori, Sci. Rep. **4**, 5535 (2014).
- [13] T. Mao and Z. D. Wang, arXiv:1403.4365; Phys. Rev. A **91** (to be published).
- [14] D. Marcos, P. Rabl, E. Rico, and P. Zoller, Phys. Rev. Lett. **111**, 110504 (2013).
- [15] L. García-Álvarez *et al.*, arXiv:1404.2868.
- [16] J. Q. You and F. Nori, Nature **474**, 589 (2011).
- [17] M. H. Devoret and R. J. Schoelkopf, Science **339**, 1169 (2013).
- [18] A. A. Houck, H. E. Türeci, and J. Koch, Nature Phys. **8**, 292 (2012).
- [19] S. Schmidt and J. Koch, Annalen der Physik **525**, 395 (2013).
- [20] J. Koch *et al.*, Phys. Rev. A **76**, 042319 (2007).
- [21] J. A. Schreier *et al.*, Phys. Rev. B **77**, 180502 (2008).
- [22] Y. Chen *et al.*, Phys. Rev. Lett. **113**, 220502 (2014).
- [23] M. R. Geller *et al.*, arXiv:1405.1915.
- [24] X. Y. Jin *et al.*, arXiv:1412.2772 (2014).
- [25] R. Barends *et al.*, Phys. Rev. Lett. **111**, 080502 (2013).

- [26] The bosonization inherits topological protection against local fluctuations seen from the fermionic system of Eq.(2), because the locality of the three forms of physical perturbations ($b_j^\dagger b_{j+1}$, $b_{j+1} b_j$, $b_j^\dagger b_j$) in the bosonic system remains unchanged after fermionization.
- [27] Supplemental Material.

- [28] Note that turning on or off these coupling parameters does not have any impact on the total ground state energy as MZMs have no contributions to the energy, namely, the total energy is conserved under these operations in the ground state, with the TRS being also preserved.

Supplemental Material

In this supplemental material, we detail the derivation of DDM pulses and the consequent effective Hamiltonian. Here we exploit the dispersive coupling mechanism which states that, for a system governed by a fast oscillating Hamiltonian $Ae^{i\omega t} + Be^{-i\omega t}$ with $\|A\|, \|B\| \ll \omega$, its evolution can be described by the effective Hamiltonian $H^{\text{Eff}} = [A, B]/\omega$ [1] (here the norm $\|O\|$ of an operator O is defined as the square root of the largest eigenvalue of $O^\dagger O$). Our basic idea is that, if we are able to use the $A = b_j^\dagger \bar{b}_j$ term in \mathcal{H}_j^L as A and the $\bar{b}_j^\dagger b_{j+1}^\dagger$ and $\bar{b}_j^\dagger b_{j+1}$ terms in $\bar{\mathcal{H}}_j^L$ as B , the resulting commutators $[A, B]$ provide the required $b_j^\dagger b_{j+1}^\dagger \bar{P}_j$ and $b_j^\dagger b_{j+1} \bar{P}_j$ terms. For this purpose we adopt the rotating frame for which \mathcal{H}_j^L and $\bar{\mathcal{H}}_j^L$ take the forms

$$\begin{aligned}\mathcal{H}_j^L &= V_j \left(b_j^\dagger \bar{b}_j^\dagger e^{i\epsilon t} + b_j^\dagger \bar{b}_j e^{i\delta t} + b_j \bar{b}_j^\dagger e^{-i\delta t} + b_j \bar{b}_j e^{-i\epsilon t} \right), \\ \bar{\mathcal{H}}_j^L &= \bar{V}_j \left(\bar{b}_j^\dagger b_{j+1}^\dagger e^{i\epsilon t} + \bar{b}_j^\dagger b_{j+1} e^{-i\delta t} + \bar{b}_j b_{j+1}^\dagger e^{i\delta t} + \bar{b}_j b_{j+1} e^{-i\epsilon t} \right).\end{aligned}\quad (9)$$

As being noticed already, the four terms in \mathcal{H}_j^L and $\bar{\mathcal{H}}_j^L$ oscillate with frequencies $\epsilon, \delta, -\delta$ and $-\epsilon$, respectively. Meanwhile, the dynamic modulation of $V_j(t)$ and $\bar{V}_j(t)$ can synthesize the dispersive coupling by shifting the frequencies of the terms in Eq. (9) upward and downward. For the modulation $V_j(t) = 2t_j \cos(\eta - \delta)t + 2q_j \cos(\eta - \epsilon)t$, we find that $\mathcal{H}_j^P = t_j b_j^\dagger \bar{b}_j + q_j \bar{b}_j^\dagger b_j$ is positively activated (i.e. it oscillates with frequency η) and its Hermitian conjugate $\mathcal{H}_j^N = t_j \bar{b}_j b_j^\dagger + q_j b_j \bar{b}_j^\dagger$ is negatively activated. The other terms in \mathcal{H}_j^L are de-activated because their frequencies are far away from the dispersive active region $[-\eta, \eta]$ at least by the order of δ . Also, for the modulation $\bar{V}_j(t) = 2\bar{t}_j \cos(\eta - \delta)t + 2\bar{q}_j \cos(\eta + \epsilon)t$, we can positively activate $\bar{\mathcal{H}}_j^P = \bar{t}_j \bar{b}_j b_{j+1}^\dagger + \bar{q}_j \bar{b}_j b_{j+1}$ and negatively activate $\bar{\mathcal{H}}_j^N = \bar{t}_j \bar{b}_j^\dagger b_{j+1} + \bar{q}_j \bar{b}_j^\dagger b_{j+1}^\dagger$. The dispersive coupling between \mathcal{H}_j^L and $\bar{\mathcal{H}}_j^L$ results in two effects. The first is the self part

$$([\mathcal{H}_j^P, \mathcal{H}_j^N] + [\bar{\mathcal{H}}_j^P, \bar{\mathcal{H}}_j^N])/\eta$$

which contains the self-energy corrections of the sites $(j, +)$, $(j, -)$, and $(j+1, +)$. The more nontrivial terms emerge from the mutual dispersive coupling

$$([\mathcal{H}_j^P, \bar{\mathcal{H}}_j^N] + [\bar{\mathcal{H}}_j^P, \mathcal{H}_j^N])/\eta$$

which can be simplified as

$$\mathcal{H}_j^{\text{Eff}} = \frac{t_j \bar{t}_j}{\eta} b_j^\dagger b_{j+1}^\dagger \bar{P}_j + \frac{t_j \bar{q}_j}{\eta} b_j^\dagger b_{j+1}^\dagger \bar{P}_j + \text{h.c.} \quad (10)$$

Similarly, the dispersive coupling between the $(j, -) \longleftrightarrow (j+1, +)$ and $(j+1, +) \longleftrightarrow (j+1, -)$ links provides the effective $(j, -) \longleftrightarrow (j+1, -)$ coupling

$$\bar{\mathcal{H}}_j^{\text{Eff}} = -\frac{\bar{t}_j t_{j+1}}{\eta} \bar{b}_j^\dagger \bar{b}_{j+1} P_{j+1} - \frac{\bar{t}_j q_{j+1}}{\eta} \bar{b}_j^\dagger \bar{b}_{j+1}^\dagger P_{j+1} + \text{h.c.} \quad (11)$$

Notice that all the effective hopping and pairing constants in Eqs.(10) and (11) can be independently controlled by the pumping parameters (t_j, q_j) and (\bar{t}_j, \bar{q}_j) . Through the setting

$$\begin{aligned}t_j &= (-1)^{j-1} t, q_j = (-1)^{j-1} q, \\ \bar{t}_j &= (-1)^{j-1} \bar{t}, \bar{q}_j = (-1)^{j-1} \bar{q}, \bar{q}/\bar{t} = -q/t,\end{aligned}\quad (12)$$

the population-dependent phase terms in the bosonic version of H_{DIII} can be directly reproduced from Eqs. (10) and (11).

* huyong@hku.hk

† zwang@hku.hk

[1] S. B. Zheng and G. C. Guo, Phys. Rev. Lett. **85**, 2392 (2000).
